

# Thermal, electrical and optical properties of phosphine metal complex including Ni

DUYGU YAZICI<sup>a</sup>, HAKAN GÜNDOĞMUŞ<sup>a,b</sup>, BEKİR ÖZÇELİK<sup>a,\*</sup>, OSMAN SERINDAĞ<sup>c</sup>

<sup>a</sup>Department of Physics, Faculty of Arts and Sciences, Çukurova University 01330 Adana, Turkey

<sup>b</sup>Faculty of Engineering, Hakkari University. 30000 Hakkari, Turkey

<sup>c</sup>Department of Chemistry, Faculty of Arts and Sciences, Çukurova University 01330 Adana, Turkey

The structural, thermal, electrical and optical properties of the phosphine metal complex including Ni have been investigated. SEM results show that the sample has a granular structure together with some voids. The complex is electrically insulator at room temperature, however, the electrical conductivity increases as the temperature increases from ~366 K with the value of  $1.4 \times 10^{-11}$  S/cm, indicating its semiconducting behavior. The electrical conductivity result shows three conduction regions according to the temperature. The thermal activation energies are 0.70 eV and 0.60 eV for extrinsic and intrinsic region, respectively. Optical absorption studies in the wavelength range of 200-1100 nm at room temperature show that optical band gap  $E_g$  of Ni(PPh<sub>3</sub>)Cl<sub>2</sub> metal complex is 2.35 eV. It is determined that direct transitions are responsible for optical absorption. The refractive index and extinction coefficient of complex are determined in the visible range as a function of wavelength. The differences in the optical constants are observed in the investigated wavelength ranges.

(Received August 8, 2013; accepted January 22, 2014)

**Keywords:** Phosphine metal complexes, Electrical properties, Optical properties

## 1. Introduction

In recent years, a great deal of experimental work has been done on materials related to organic and inorganic solid state [1-7]. Research on the metal complex is being known as an interdisciplinary field of study, which combines related work not only by chemists and physicists but also by biologists and medical researchers. Transition metal phosphine complexes have been of interest for many years in terms of their importance in organic synthesis [8,9] as well as their medical properties including anti-tumor and anti-microbial activities [10-12] and catalytic performance [13].

Optical properties of metal complex are recently intensively investigated because of the interesting properties of their crystallized layers, considerably different from the properties of free molecules. The optical and electrical properties of these materials can be significantly different from those of single crystals or molecules in solution. Therefore, in order to enhance the information on organic and inorganic solid state, better knowledge of structure and optical properties of their layers is needed. Moreover, it is necessary to determine the physical parameters such as electrical, thermal conductivity, absorption, transmission, refraction, energy gap, oscillator and dispersion energies, dielectric constants, etc. of metal complex.

While the chemistry of triaryl phosphine and their metal complexes have been deeply studied [14], but their physical properties have not been sufficiently studied. Therefore, some research groups have focused upon their

attention on metal complexes of organic and inorganic solid state.

In this study, we have investigated the microstructure, temperature dependence of electrical conductivity and optical properties of Ni(PPh<sub>3</sub>)Cl<sub>2</sub> metal complex.

## 2. Experimental process

Ni(PPh<sub>3</sub>)Cl<sub>2</sub> metal complex were prepared by the similar procedure as mentioned Ref. [15]. PPh<sub>3</sub> (Sigma Aldrich, 99%, 5.25 g, 0.002 mol) was added into a solution of NiCl<sub>2</sub>·6H<sub>2</sub>O (Sigma Aldrich, 99%, 2.38 g, 0.001 mol) in ethanol (20 mL). The mixture was refluxed for 40 minute to give a dark blue-green solid product. The solid was filtered off, washed with ethanol and dried under vacuum. The yield is 5.6 g (%86).

The microstructural characterization of the sample (on polished surface) was performed using Leo EVO-40 VPX Scanning Electron Microscope (SEM) with a LEO EVP-40xVPX apparatus.

The thermal behavior of the Ni(PPh<sub>3</sub>)Cl<sub>2</sub> metal complex was investigated using a Perkin Elmer Sapphire DSC and Perkin Elmer Pyris Diamond TG/DTA. The instrument was calibrated using the melting point of high purity indium. All the DSC and TG/DTA experiments were performed with ~10 mg powder samples taken in crimped aluminum pans under air. The DSC and TG/DTA curves were recorded in the temperature range of 20-250 and 20- 550 °C, respectively, for heating rates of 20 °C/min.

The sample were prepared in the form of pellets, which have 0.86 mm thickness and 6 mm radius, under a pressure of approximately  $2 \times 10^7$  Pa. Then, the silver paint was applied by brushing the two ends of the pellet in order to make proper electrical contact. The electrical conductivities of the sample with respect to the temperature were measured by using a two probe method, with a Keithley 6514 system electrometer and a DC Keithley 230 programmable voltage source.

For optical measurements, the sample was thoroughly ground and pressed into circular discs of 13 mm diameter at a pressure of approximately  $1 \times 10^7$  Pa. Optical absorption and transmittance spectra of the sample were recorded using a Perkin Elmer Lambda 2S (double beam) spectrophotometer in the wavelength range 200-1100 nm.

### 3. Results and discussions

It has been obtained that the weight loss of sample occurs in a single step by means of the thermo-gravimetric measurements. The sample has shown good thermal stability until 200 °C and the decomposition started gradually in the range of 200-250 °C at which an exothermic peak occurred at the heat-flow curve, then % 80 percent of the sample was lost at 350 °C. From the DSC (differential scanning calorimeter) measurements, the small endothermic peaks due to the losing of the crystal water in the structure and an exothermic peak around 233 °C corresponding to the onset temperature of decomposition of phosphine were observed.

The scanning electron micrograph of the  $\text{Ni}(\text{PPh}_3)\text{Cl}_2$  metal complex has been presented in Fig.1. It can be seen that the grains are regularly dispersed and, have an irregular sizes and some voids. Therefore, the electrical conductivity of the sample is probably affected by such a kind of structure.

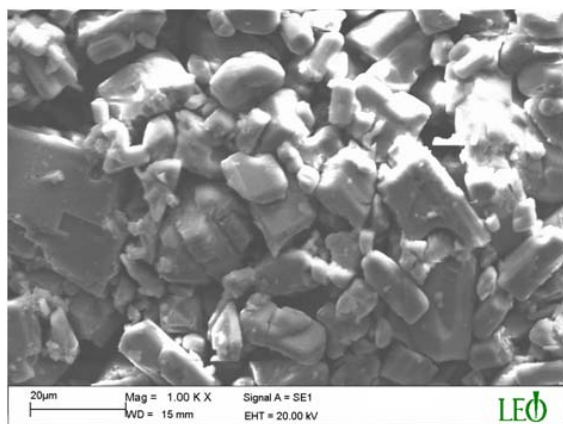


Fig. 1. SEM photograph of  $\text{Ni}(\text{PPh}_3)\text{Cl}_2$  sample.

We have found out by hot probe measurement that  $\text{Ni}(\text{PPh}_3)\text{Cl}_2$  complex shows n-type electrical conductivity, i.e. the most of the carriers are electrons. According to

Arrhenius theory, for semiconductors, a plot of electrical conductivity versus temperature is given by the equations [16]:

$$\sigma = \sigma_0 \exp[-E_a/kT] \quad (1)$$

where  $\sigma_0$  is the pre-exponential factor,  $E_a$  is the thermal activation energy for the electrical conductivity and  $k$  is the Boltzmann's constant. The electrical conductivity variations with temperature of a pellet shaped  $\text{Ni}(\text{PPh}_3)\text{Cl}_2$  complex have measured, and  $\ln\sigma$  versus  $1000/T$  graph was exhibited in Fig.2. It can be seen that  $\text{Ni}(\text{PPh}_3)\text{Cl}_2$  complex shows three distinct regions depending on the increase of temperature. The extrinsic conductivity occurs at low temperatures, while the intrinsic conductivity occurs at high temperatures. The extrinsic and intrinsic regions have a positive temperature coefficient of electrical conductivity. It means that the increasing of electrical conductivity with respect to reciprocal temperature is linear and starts as soon as the charge carriers have enough activation energy. In addition, the electrical conductivity starts around 366 K and the complex exhibits three conductivity regions. As can be seen in the first (I) and third (III) regions the electrical activation energy of sample has positive values, but the second (II) region is saturation region. The electrical conductivity increases with the increasing temperature in region I, showing activation from the donor level to the conduction band (extrinsic behavior). This behavior is well expressed by semiconducting character with thermal activation energy,  $E_a$ , through Eq.1.  $E_a$  is calculated as 0.70 eV by means of slope of conductivity curve. Therefore, at low temperatures the  $\ln\sigma$  versus  $1000/T$  curve will again be straight line.

In region II, the stabilization of conductivity with the increasing temperature is attributed to scattering of carriers by phonons due to lattice vibrations [16-18]. The slope of line and its temperature range change generally depending on the structure of the sample.

In region III, the electrical conductivity has a positive coefficient with activation energy higher than that of region I. In this region (intrinsic region), an activation takes place from the valance band to the conduction band [3,6,19]. The high activation energy value is probable related to electronic band-band transition. The energy band gap related to this region was calculated as  $E_g = 1.2$  eV. The mobilities of the carriers also enhance during increase of temperature. This, again, points out a typical semiconductor behavior.

As it has been discussed above, the dc-electrical conductivity behaves in accordance with Arrhenius law. This behavior is explained in terms of the hopping conducting mechanism in which the electron or hole hops from a localized site to the next one, and causes to change the position of the surrounding ions. Then it is trapped temporarily in an excited state. The electron resides at its new site until it is thermally activated to migrate to another nearby site. Another aspect of charge hopping mechanism is that either electrons on the negative ions or the holes left behind on the positive ions tend to affect the local defects.

So, the activation energy arises for charge transport [16,20-22].

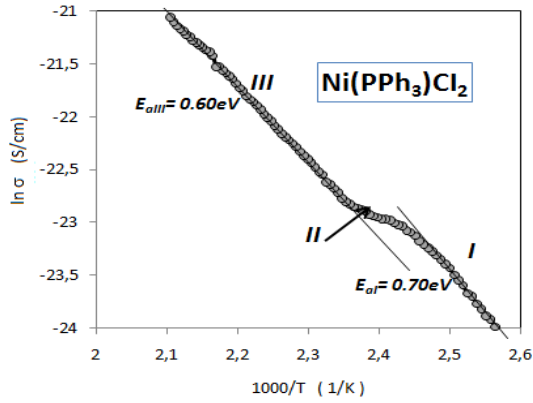


Fig. 2. Temperature dependence of electrical conductivity of Ni(PPh<sub>3</sub>)Cl<sub>2</sub> sample.

The optical absorbance and transmittance spectra were measured with UV+VIS spectroscopy. The optical absorbance spectrum as a function of wavelength was shown in Fig. 3. It is seen that the absorbance spectrum increases rapidly with decreasing wavelength and passes a maxima around 420 nm. The linear absorption coefficient  $\alpha$  was calculated using

$$\alpha = [2.3 (\text{abs})]/d \quad (2)$$

where  $d$  is the sample thickness. The optical band gap of the sample was determined from the relation between the absorption coefficient and the incident photon energy given as [16, 23]:

$$\alpha h\nu = A(h\nu - E_g)^n \quad (3)$$

where  $A$  is a constant,  $h$  is Planck's constant,  $\nu$  is the frequency,  $E_g$  is the optical energy gap between the valance band and conduction band, and  $n$  depends on the kind of prevailing optical transition. Specifically,  $n$  takes 1/2, 3/2, 2, and 3 values for transitions directly allowed, directly forbidden, indirectly allowed and indirectly forbidden, respectively. By using the values of absorption data exhibited in Fig. 3, we have plotted  $(\alpha h\nu)^2$  versus photon energy ( $h\nu$ ). As can be seen from the inset graph of Fig. 3, the optical band gap,  $E_g$ , is obtained as 2.35 eV.

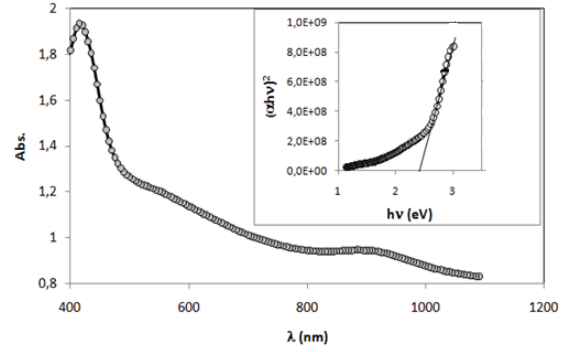


Fig. 3. Optical absorbance spectra versus wavelength and plot of  $(\alpha h\nu)^2$  versus  $(h\nu)$  (inset figure).

The relation between the absorbance, transmittance and reflectance is given as:

$$T = (1 - R)^2 \exp(-\alpha d) \quad (4)$$

where  $T$  and  $R$  are the transmittance and the reflectance, respectively. If one consider the air as first medium and the sample as second medium, the reflectance  $R$  is written as;

$$R = \frac{(n-1)^2 + k^2}{(n+1)^2 + k^2} \quad (5)$$

where  $n$  is the refractive index and  $k$  is the extinction coefficient. If  $k^2 \ll (n-1)^2$ ,  $n$  is given as:

$$n = \frac{(1 + R^{1/2})}{(1 - R^{1/2})} \quad (6)$$

The calculated values of the refractive index  $n$  in the present spectral region 400-1100 nm are illustrated in Fig. 4. A tendency to decrease at the refractive index value is observed with increasing wavelength.

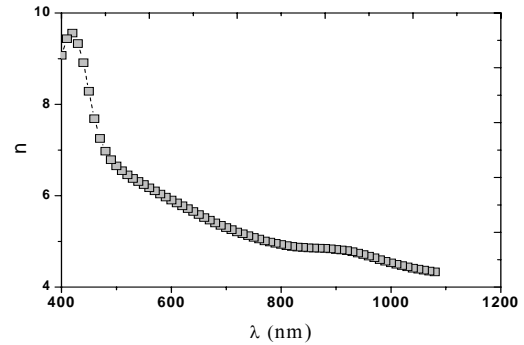


Fig. 4. The variation of refractive index with respect to photon wavelength.

The values of single oscillator energy,  $E_0$ , and the electronic dispersion energy,  $E_d$ , can be calculated from the intercept and the slope of the fitted to straight line  $[(n^2 - 1)]^{-1}$  versus  $(h\nu)^2$  plots as shown in Fig.5, which satisfies Wemple and Didomenico formula [24, 25].

$$n^2(h\nu) - 1 = \frac{E_d E_0}{E_0^2 - (h\nu)^2} \quad (7)$$

where  $n(h\nu)$  is the refractive index at photon energy. The values of  $E_0$  and  $E_d$  are estimated as 2.99 eV and 51.7 eV, respectively.

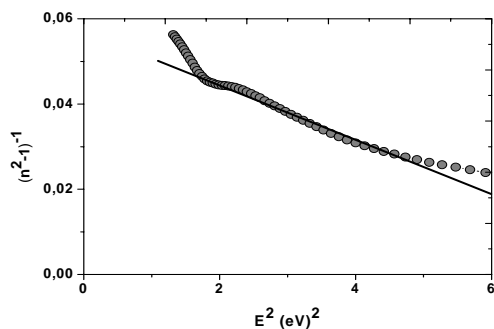


Fig. 5. The variation of  $(n^2 - 1)^{-1}$  versus  $E^2$ .

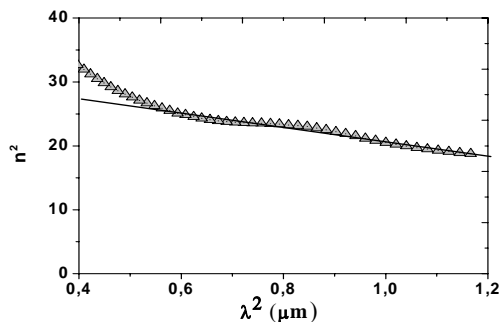


Fig. 6. The graph of  $n^2$  versus  $\lambda^2$ .

The dielectric constant is partially due to free electrons and partially due to bound electrons as represented by following relation; [26]

$$n^2 = \varepsilon_L - [(e^2 / \pi c^2)(N / m^*)]\lambda^2 \quad (8)$$

where,  $e$  is the electron charge,  $c$  is the light speed,  $\lambda$  is the light wavelength,  $\varepsilon_L$  is the lattice dielectric constant and  $(N/m^*)$  is the ratio of carrier concentration to its effective mass. Fig. 6 represents the dependence of  $n^2$  as a function of  $\lambda^2$  for the Ni(PPh<sub>3</sub>)Cl<sub>2</sub> complex. The value  $(N/m^*)$  is determined from the slope of the linear part of graph. The

values of  $(N/m^*)$  and  $\varepsilon_L$  are determined to be  $1.46 \cdot 10^{49} \text{ gm}^{-1} \text{ cm}^{-3}$  and 32.57, respectively.

We have also calculated the real ( $\varepsilon_1$ ) and imaginary parts ( $\varepsilon_2$ ) of optical dielectric constant by using the following equations:

$$\varepsilon_1 = n^2 - k^2 \quad (9)$$

$$\varepsilon_2 = 2nk \quad (10)$$

The graphs of  $\varepsilon_1$  and  $\varepsilon_2$  were represented in Fig. 7. Both real and imaginary parts of optical dielectric constant show peaks around 3 eV.

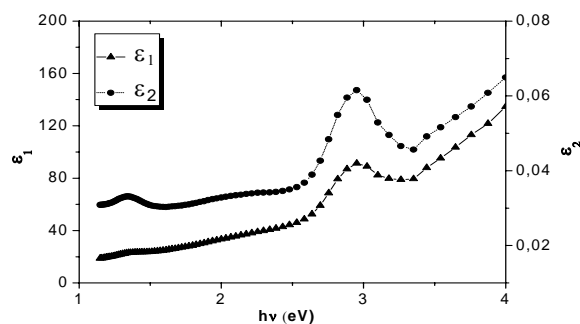


Fig. 7. The variation of real and imaginary parts of dielectric constant versus energy.

#### 4. Conclusion

The structural, thermal, electrical and optical properties of the Ni(PPh<sub>3</sub>)Cl<sub>2</sub> complex has been investigated. The complex shows typical semiconducting characteristics, acts as n-type semiconductor. The electron transport in investigated complex is influenced by its molecular structures.

The mechanism of optical absorption follows the rule of direct transition. The spectral dependence of the optical constants indicate that both refractive and extinction coefficient increases with photon energy.

#### References

- [1] W. J. Liu, G. X. Xiong, W. P. Wang, Applied Organometallic Chemistry, **21**, 83, (2007).
- [2] A. El-Shekeil, M. A. Khalid, H. Al-Maydama, A. Al-Karbooly, European Polymer Journal, **35**, 575, (2001).
- [3] A. Yassar, F. Demanze, D. Fichou, Optical Materials, **12**, 379, (1999).
- [4] S. Sarkar, Y. Aydogdu, F. Dagdelen, B. B. Bhaumik, K. Dey, Materials Chemistry and Physics, **88**, 357, (2004).
- [5] F. Dagdelen, M. Koca, C. Kırılmış, Y. Aydogdu, Sixth International Conference of the Balkan Physical

- Union, 581, (2007).
- [6] Y. Aydogdu, F. Yakuphanoglu, F. Dagdelen, M. Sekerci, I. Aksoy, *Mat. Lett.* **57**, 237 (2002).
- [7] F. Yakuphanoglu, F. Dagdelen, Y. Aydogdu, A. Aydogdu, M. Sekerci, *Mat. Lett.*, **57**, 3330 (2003).
- [8] D. Gelman, H. Schumann, J. Blum, *Tetrahedron Letters* **41**, 7555 (2000).
- [9] R. Daniel Palo, C. Erkey, *J. Chem. Eng. Data* **43**, 47 (1998).
- [10] K. Nomiya, R. Noguchi, K. Ohsawa, K. Tsuda, M. Oda, *Jour. Inorg. Biochem.* **78**, 363 (2000).
- [11] N. Chikaraishi, K. Sekino, C. Koumo, N. Shimada, M. Ishikawa, K. Nomiya, *Jour. Inorg. Biochem.*, **84**, 55 (2001).
- [12] N. Manav, A. K. Misha, N. K. Kaushik, *Spectrochimica Acta Part A* **60**, 3087 (2004).
- [13] W. Sizhong, L. Shiwei, *Applied Catalysis A: General* **246**, 295 (2003).
- [14] W. Dew Horrocks, E. S. Greenberg, *Inorganic Chemistry*, **10**, 2190 (1971).
- [15] J. R. Blacburn, R. Nardberg, F. Stevie, R. G. Albridge, M. M. Jones, *Inorg.Chem.*, **9**, 2374 (1970).
- [16] N. F. Mott, E. A. Davis, *Electronic Processes in Non-Crystalline Materials*, Clarendon Pres, Oxford, (1971).
- [17] M. S. Masoud, S. A. El-Enein, E. El-Shereafy, *J. Therm. Anal.* **37**, 365 (1991).
- [18] M. S. Masoud, E. A. Khalil, M. E. Kassem, *React.Solids* **2**, 269 (1986).
- [19] Y. Aydogdu, F. Yakuphanoglu, A. Aydogdu, E. Tas, A. Cukurovali, *Materials Letters*, **57**, 3755 (2003),
- [20] D. F. Shriver, P. W. Atkins, C. H. Langford, *Inorganic Chemistry*, Oxford Univ. Press, Oxford (1996).
- [21] A. J. Epstein, H. Rommelmann, M. Abkowitz, H. W. Gibson, *Mol. Crys. Liq. Crys.* **77**, 81 (1981).
- [22] F. Purcell, C. Kotz, *Inorganic Chemistry*, Saunders, New York, (1977)
- [23] F. Urbach *Phy. Rev.* **92**, 1324 (1953).
- [24] S. H. Wemple, M. Didomenico, *J. Phys. Rev. B*, **3**, 1338 (1971).
- [25] S. H. Wemple, M. Didomenico, *J. Phys. Rev. B*, **3**, 13767 (1973).
- [26] M. M. El-Nahass, A. A. M. Farag, E. M. Ibrahim, S.Abd-El-Rahman, *Vacuum* **72**, 45 (2004).

---

\*Corresponding author: ozcelik@cu.edu.tr